Platinum nanocrystals supported by silica, alumina and ceria: metal–support interaction due to high-temperature reduction in hydrogen

S. Penner[1*], D. Wang[2], D.S. Su[2], G. Rupprechter[2], R. Podloucky[3], R. Schlögl[2], K. Hayek[1]

[1] Institut für Physikalische Chemie, Leopold-Franzens-Universität, Innrain 52a, A-6020 Innsbruck, Austria
[2] Department of Inorganic Chemistry, Fritz-Haber-Institute of the MPG, Faradayweg 4-6, 14195 Berlin, Germany
[3] Center for Computational Materials Science & Universität Wien, Liechtensteinstr. 45, A-1090 Vienna, Austria

[*] Corresponding author: e-mail simon.penner@uibk.ac.at, phone +43 512 507 5066, fax +43 512 507 2925

Abstract

Regular Pt nanoparticles, obtained by epitaxial deposition on NaCl surfaces, were supported by thin films of silica, alumina and ceria and subjected to hydrogen reduction at temperatures up to 1073 K. The changes in morphology and composition were followed by (HR)TEM, electron diffraction and EELS, and the results were supported by theoretical calculations. The structural changes of the Pt particles upon reduction at 773 K and above are surprisingly similar despite the differing chemical properties of the three supports. Some platelet- and cube-like geometries exhibit double lattice periodicities in high resolution images and electron diffraction patterns. With increasing reduction larger aggregates of more complex appearance and structure are formed. Surface reconstruction under hydrogen and alloy formation are considered as responsible for this effect. Most likely, the first step is identical on all three systems and consists in the topotactic formation of Pt rich Pt_3Me (Me = Si, Al, Ce) under the influence of hydrogen, followed by transformation into diverging structures of lower Pt content and different crystallography. Density functional calculations were performed for deriving energies of formation of PtMe and Pt_3Me compounds.

Keywords: Platinum, electron microscopy, surface reconstruction, alloy, catalysis

Introduction

In heterogeneous catalysis model systems are invaluable tools for resolving the mechanism of structure-sensitive reactions. Lately, noble metal nanocrystals grown epitaxially on NaCl and integrated into different supporting films have been successfully studied as model systems for supported catalysts [1,2]. Regular metal particles partly embedded in thin planar supports facilitate the characterisation by electron microscopy and provide a defined initial state for subsequent structural alterations due to oxidation and reduction. They are also well suited to study the influence of different supports on identical nanoparticles.

Noble metals in combination with a reducible oxide (e.g. ceria) are known to undergo metal-support interaction which may strongly influence the catalytic activity in various chemical reactions. This usually occurs under high-temperature treatment in hydrogen and is manifest either as a change of the structure and surface area of the oxide and/or the metal ("geometric effect") or as an "electronic" (chemical) interaction between the metal and the (partially) reduced oxide [3]. However, structural and chemical changes on (and of) non-reducible supports like alumina and silica upon reduction at ≥773 K have also been reported [4]. Since the described thin film model catalysts allow to investigate systems containing different supports but identical metal particles, the present work was dedicated to the structural and morphological changes of both non-SMSI and SMSI systems (Pt supported by alumina, silica and ceria) subjected to various activation procedures. Systematic series of reduction were performed in the temperature range between 673 and 1073 K. The resulting changes were followed with electron

Platinum nanocrystals supported by silica, alumina and ceria: metal–support interaction due to high-temperature reduction in hydrogen, S. Penner et al., Surface Science, accepted 10 October 2002

2

microscopy and related techniques (TEM, HRTEM, TED and EELS) and interpreted by means of density functional calculations.

Experimental

Pt particles (mean size 10 to 15 nm) were epitaxially grown on vacuum-cleaved (001) NaCl single crystal surfaces and on fresh deposited NaCl thin films. The metal was deposited at 673 K by electron beam evaporation at 10^{-6} mbar pressure (the nominal metal coverage of the NaCl surface was 2,5 - 3 nm). The samples were then covered with a supporting film of amorphous silica or alumina or of crystalline ceria (15 to 25 nm thick), prepared by reactive deposition in 10^{-4} mbar oxygen of SiO, aluminium metal and cerium oxide, respectively. Subsequently, the NaCl was dissolved in water and the films were mounted on gold EM grids [1]. After oxidation (O_2, 673K, 1h) the samples were exposed to H_2 between 673 and 1073 K for 1h, either in a flow system or in a circulating batch reactor. Their morphology and structure were examined by HRTEM and compared to the as-grown state. The images were taken with a Zeiss EM 10C, with a Philips CM FEG 200 and with a JEOL 4000 microscope. EELS measurements were performed at the Philips CM FEG 200 equipped with a Gatan energy filter.

Results

For a comparison of structural and morphological changes due to reduction the initial state has to be well defined. Fig. 1a shows a low-magnification image of as-deposited Pt particles supported by a silica film (25 nm thick). The high metal loading of the NaCl surface has resulted in large (mean diameter 12 nm) and relatively closely spaced particles. Most exhibit square or rectangular shapes and are identified as (truncated) half octahedra by weak-beam dark field imaging (Fig. 1b) [1]. The SAED pattern (insert in Fig.1a) confirms their almost perfect orientation with respect to the original NaCl substrate. Most of the particles are in their [100] zone and no Pt(111) reflections are detected. The high-resolution image of octahedral particles (insert) shows Pt (200) lattice fringes (d_{200}(Pt) = 1,96Å) rotated 45° with respect to the particle edges. Subsequent oxidation (1 bar O_2, 673K, 1h) and low-temperature reduction (1 bar H_2, T ≤ 673K, 1h) does not lead to significant changes, except for the appearance of higher-indexed facets, generally observed as particle „rounding" in low-resolution images [1].

Reduction at ≥773 K leads to a quite different picture. Fig. 2a shows Pt particles on silica after a reductive treatment at 873K. Most particles have changed shape and orientation. While one fraction has increased in size, obviously by coalescence, a considerable number of particles exhibit a characteristic cube or platelet shape with sharp edges. The corresponding SAED pattern (insert) still shows distinct, but broadened Pt spots, but also series of rings. Thus, some particles have changed their azimuthal orientation, but are still in [001] zone. Apart from (200) and (220), also (111) and (311) reflections belonging to a [110] zone can be detected,
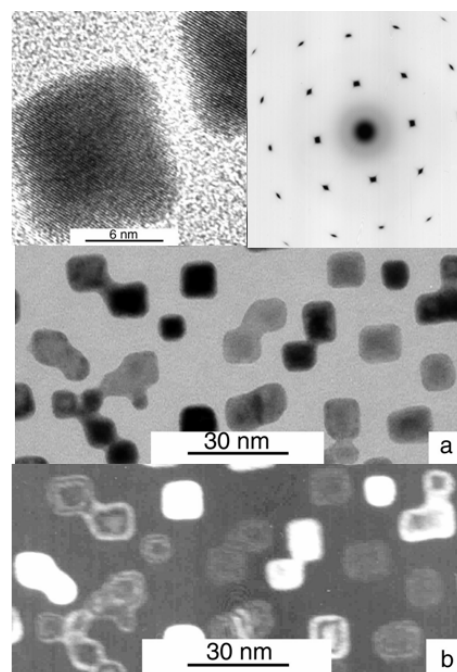

Fig. 1: As-grown Pt particles supported by SiO_2 (a) bright-field, (b) weak-beam dark field image. Inserts: HREM image of an octahedral Pt particle and selected area diffraction pattern.
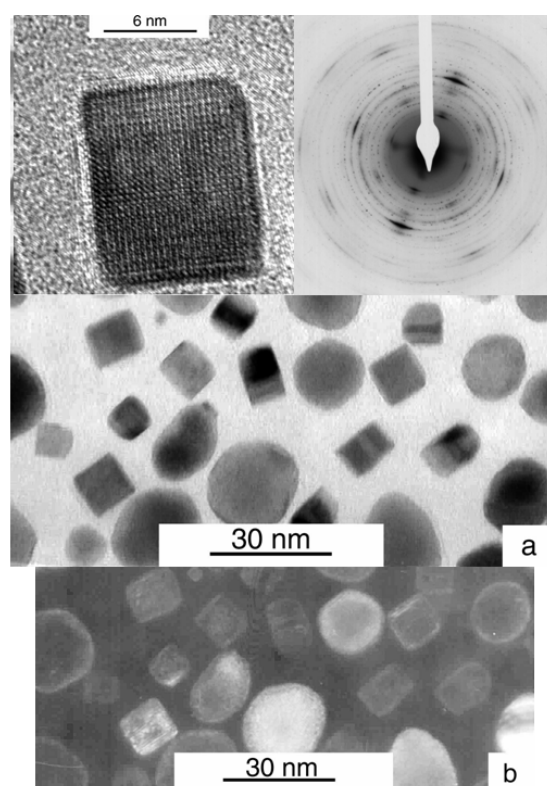

Fig. 2: Pt particles on silica after reduction in H_2 at 873K for 1h. (a) bright-field, (b) dark field. Left insert: HREM

which suggests a change of base planes of some particles. Additional weaker spots coincide with forbidden (100) and image of a cube-shaped particle. Right insert: electron diffraction pattern.

(110) Pt reflections, but can be attributed to Pt_3Si with a primitive cubic (Cu_3Au) structure (a = 3,89Å). (Table 1) [5]. Moreover, the high-resolution images of particles with sharp edges (insert) reveal periodicities parallel to these edges which may be regarded either as a doubling of the (200) distance of fcc Pt ($2 \times d_{200}(Pt) = 3,92$Å), or as arising from Pt_3Si (3,89Å). Further reflections in the diffraction pattern may arise from hexagonal low-temperature quartz ([6] and/or from other silicide modifications (see below) cf. Table1). In the corresponding dark-field images (Fig. 2b) no characteristic fringes due to thickness variations are detected, hence most particles have changed from truncated octahedra to cube or platelet like structures. This phase transformation is reversed upon heating in oxygen in 673 K for 1 h. Subsequent reduction in hydrogen at 673 - 873 K re-establishes the previous state as documented by electron diffraction: Upon oxidising the "HTR" phase all reflections except those of the fcc Pt structure vanish, but they reappear after HTR. However, with increasing reduction temperature and time more "agglomerated" and rounded particles are observed and the diffraction pattern becomes more and more complex. A detailed analysis [7] indicates the formation of monoclinic Pt_3Si (denoted by "m" in table 1) and of silicon richer structures like $Pt_{12}Si_5$. Analogous reduction experiments have been performed with a Pt/alumina thin film containing originally identical Pt particles (mean size 10 nm, thickness of alumina 15 nm). The as-deposited alumina is amorphous, but may crystallise in the electron beam and during oxidation and reduction. Fig. 3 shows the catalyst after reduction to 873 K together with a SAED pattern and

Table 1: Experimental interplanar distances d_{hkl} [Å] and possible correlation to Pt_3Si (cubic), Pt_3Si (monoclinic), $Pt_{12}Si_5$, and Pt_3Al.

| Exp. distances d_{hkl} Pt_xSi_y [Å]	Assignment	Exp. distances d_{hkl} Pt_xAl_y [Å]	Assignment
3,91	Pt_3Si (c) (100) or Pt_3Si (m) (002)	3,92	Pt_3Al (100)
3,45	γ-SiO_2 (101) or $Pt_{12}Si_5$ (301)		
3,00	$Pt_{12}Si_5$ (420)	2,95	
2,76	Pt_3Si (c) (110) or Pt_3Si (m) (202) or $Pt_{12}Si_5$ (331)	2,79	Pt_3Al (110)
2,69	Pt_3Si (m) (-202)	2,61	
2,46	γ-SiO_2 (110)		
2,36	Pt_3Si (m) (113) or $Pt_{12}Si_5$ (222)	2,29	Pt(111) or γ-Al_2O_3
2,20	Pt_3Si (c) (111) or Pt_3Si (m) (-222)	2,19	Pt_3Al (111)
2,13	$Pt_{12}Si_5$ (620)		
1,96	Pt (200) or Pt_3Si (c)(200)	1,98	Pt_3Al (200) or Pt (200) or γ-Al_2O_3
1,81	Pt_3Si (c) (210) or Pt_3Si (m) (313) or $Pt_{12}Si_5$ (003)	1,74	Pt_3Al (210)
1,58	Pt_3Si (c) (211)	1,54	Pt_3Al (211)
1,38	Pt_3Si (c) (220) or Pt (220) or Pt_3Si (m) (404)	1,41	Pt_3Al (220) or Pt (220) or γ-Al_2O_3
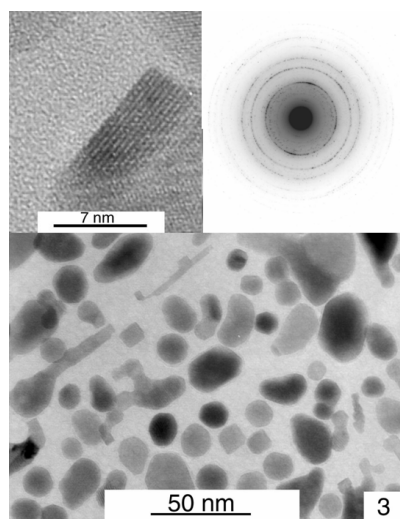
Fig. 3: Pt particles on alumina after reduction in H_2 at 873K for 1h. Left insert: HREM image of a cube-like particle. Right insert: electron diffraction pattern.

the high-resolution image of a selected particle. Apart from larger (agglomerated) and "round" aggregates many particles have developed similar cube or platelet-like structures as on silica, again in contrast to the original octahedral shape. The electron diffraction pattern and the HREM image (inserts) reveal again a periodicity of $3,92 \pm 0,05$Å. Apart from ring reflections arising from γ-alumina many reflections are close to those measured on the silica-supported catalyst and indicate the presence of Pt_3Al, also of Cu_3Au structure (lattice constant 3,87Å) (Table1). Again, more complex structures are formed upon reduction at higher temperature and for longer times. These are also more easily observed after adding metallic aluminium to the alumina support film before the reduction and must be attributed to more Al enriched alloy phases, particularly PtAl [8].

Quite analogous "primary" structures, i.e. cube and platelet shapes, were also observed upon reduction of the ceria-supported Pt nanocrystals between 773 and 973 K.

Again they are most likely attributed to Pt$_3$Ce, also with a Cu$_3$Au lattice (a = 4,16 Å). Here also further reduction leads to different particle habits [9], but also to changes of composition and structure of the support, as will be discussed separately [10].

Discussion and conclusions

The discussion about structural changes of Pt particles upon high-temperature hydrogen reduction has been going on for some time. Cube-like structures with sharp edges have been already reported before high-resolution EM became available [11,12], and were attributed to surface reconstruction under the influence of hydrogen, leading the system to minimum surface energy [13]. That alloy formation has to be taken into account was shown by Lamber et al. [5] who observed diffraction features compatible with Pt$_3$Si after heating a Pt/silica model catalyst in hydrogen at 840 K. Under the given experimental conditions alloy formation is thermodynamically feasible for all three described systems [14]. Density functional calculations of energies of formation and lattice parameters of some relevant PtMe and Pt$_3$Me compounds (as summarized in Table 2) were performed by

Table 2: VASP-calculated formation energies [eV] of several relevant alloys

Phase	E$_f$ [eV]	E$_f$ per atom [eV]
Pt$_3$Si	-1,201	-0,300
PtSi	-1,278	-0,639
Pt$_3$Al	-2,754	-0,689
PtAl	-2,109	-1,055
Pt$_3$Ce	-3,888	-0,972

the ab-initio approach VASP [15], and confirm the high stability of the initially formed Cu$_3$Au structures.

Hence, if we start from the pure oxide in intimate contact with the Pt metal particles, we may assume the formation of the Pt rich and stable Pt$_3$Me phase as a first step. This may, however, be initiated by a reconstruction of the original octahedral particles into cubes under hydrogen, thereby facilitating the topotactic growth of the alloy in the proper orientation. The crystallographic alignment of the original particles provides the opportunity to monitor the reorientation process. In contrast to possible hydride intermediates the resulting alloys are kinetically stable under ambient conditions.

After reduction, EELS spectra of alumina covered Pt particles show a shift of the plasmon peak by about 2 eV compared to the pure alumina support, which is also consistent with alloy formation. Conclusively, alloy formation, possibly preceded by surface reconstruction, is likely to occur in all three systems by topotactic growth of Pt$_3$Me as a first step. Possible reasons for the absence of cube-like shapes, or of alloy formation, as sometimes stated under otherwise comparable experimental conditions [16], could be the absence of a preferred relationship between Pt and support, e.g. of topotactic nuclei or kinetic inhibition, e.g. less contact area between the support and particles grown *on top* of the support.

Acknowledgement

References
[1]   G. Rupprechter, K. Hayek, L. Rendon and M. José-Yacaman, Thin Solid Films 260 (1995) 148.
[2]   K. Hayek, M. Fuchs, B. Klötzer, W. Reichl and G. Rupprechter, Top. Catal. 13 (2000) 55.
[3]   G. L. Haller, D. E. Resasco, Adv. Catal. 36 (1989) 173.
[4]   G. J. den Otter and F. M. Dautzenberg, J. Catal. 53 (1978) 116.
[5]   R. Lamber and N. Jaeger, J. Appl. Phys. 70 (1991) 457.
[6]   Powder Diffraction File 1994, PDF 2 Database 1-44, International Center for Diffraction Data.
[7]   D. Wang, S. Penner, G. Rupprechter, D.S. Su, K. Hayek and R. Schlögl, submitted to Mat. Chem. Phys.
[8]   W. Bronger, P. Müller and K. Wrzesien, Z. Anorg. Allg. Chem. 623 (1997) 362.
[9]   S. Bernal, J. J. Calvino, M. A. Cauqui, J. M. Gatica, C. Larese, J.A. Pérez-Omil and J. M. Pintado, Catal. Today 50 (1999) 175.
[10]   S. Penner D. Wang, D. S. Su, G. Rupprechter, R. Schlögl and K. Hayek, submitted to Vacuum.
[11]   T. Wang, C. Lee and L.D. Schmidt, Surf. Sci. 163 (1985) 181.
[12]   W. Romanowski and R. Lamber, Thin Solid Films 127 (1985) 139.
[13]   A.-C. Shi and R.I. Masel, J. Catal. 120 (1989) 421.
[14]   Landolt-Börnstein New Series IV/5a, IV/5c and IV/5I.
[15]   G. Kresse and J. Hafner, Phys. Rev. B 47 (1993) RC558
[16]   A.S. Ramachandran, S.L. Anderson and A.K. Datye, Ultramicroscopy 51 (1993) 282.